Eur. Phys. J. D **40**, 399–403 (2006)
DOI: 10.1140/epjd/e2006-00177-0

THE EUROPEAN PHYSICAL JOURNAL D

Momentum interferences of a freely expanding Bose-Einstein condensate due to interatomic interaction change

A. Ruschhaupt[1,a], A. del Campo[2,b], and J.G. Muga[2,c]

[1] Institut für Mathematische Physik, TU Braunschweig, Mendelssohnstrasse 3, 38106 Braunschweig, Germany
[2] Departamento de Química-Física, Universidad del País Vasco, Apdo. 644, 48080 Bilbao, Spain

Received 31 March 2006 / Received in final form 22 May 2006
Published online 28 July 2006 –

Abstract. A Bose-Einstein condensate may be prepared in a harmonic trap with negligible interatomic interactions using a Feshbach resonance. If a strong repulsive interatomic interaction is switched on and the trap is removed to let the condensate evolve freely, a time dependent quantum interference pattern takes place in the short time (Thomas-Fermi) regime, in which the number of peaks of the momentum distribution increases one by one, whereas the spatial density barely changes. The effect is stable for initial states with interactions and realistic time-dependence of the scattering length.

PACS. 03.75.-b Matter waves – 03.75.Kk Dynamic properties of condensates; collective and hydrodynamic excitations, superfluid flow – 03.75.Nt Other Bose-Einstein condensation phenomena

1 Introduction

The dynamics of Bose-Einstein condensates has been much studied, both experimentally and theoretically, for determining the properties of the condensate and its transport behaviour in waveguides or free space with potential applications in nonlinear atom optics, atom chips and interferometry. Fully free (three dimensional) or dimensionally constrained expansions have in particular been subjected to close scrutiny to obtain, from time series of cloud images and the appropriate theoretical models, information on the condensate and its confining potentials [1]. In reduced dimensions, the expansions have also been examined to characterise and identify different dynamical regimes (the mean-field dominated Thomas-Fermi limit, quasi-condensates and the dilute Tonks-Girardeau gas of impenetrable bosons [2–5]), or to investigate statistical behaviour in a partial release of the condensate into a box of finite size [6]. An effectively one dimensional (1D) Bose gas may be realized experimentally by a tight confinement of the atomic cloud in two (radial) dimensions and a weak confinement in the axial direction so that radial motion is constrained to the ground transversal state. Expansions are quite generally described and observed in coordinate space but very interesting phenomena occur in momentum space [7,8]. Also interferences, which show the wave nature of the condensate and may form the basis of metrological applications, are usually apparent in coordinate space, between independent condensates [9] or as a self-interference [10], but, as in our present case, they may be genuinely momentum space effects, possibly with an indirect and less obvious spatial manifestation. (Other striking example of quantum momentum-space interference phenomenon for an ordinary, non-condensate, one-particle wavefunction colliding with a barrier has been discussed recently [11].) The expansions may be manipulated in different ways, e.g. by controlling the time dependence and shape of the external trapping potentials or by varying the interatomic interaction using a magnetically tunable Feshbach resonance [12] or an optically induced Feshbach resonance [13].

In this paper we shall take advantage of these control possibilities and study a quantum interference effect in momentum originating from a change of the interatomic interaction strength. In Section 2 we describe the effect in 1D, in Section 3 its origin, and its stability is discussed in Section 4. Since quasi-one-dimensional condensates in elongated traps can show significant phase fluctuations — due to thermal excitations of the condensate, even at low temperatures [3,14,15] — one has to make sure that these fluctuations can be neglected in an experimental implementation. Alternatively, the momentum interference effect may be implemented in three dimensions; this is considered in Section 5. The paper will end with a summary.

2 Momentum interference pattern

Assume that an effectively 1D Bose-Einstein condensate is prepared in a harmonic trap. The condensate wave

[a] e-mail: a.ruschhaupt@tu-bs.de
[b] e-mail: qfbdeeca@ehu.es
[c] e-mail: jg.muga@ehu.es

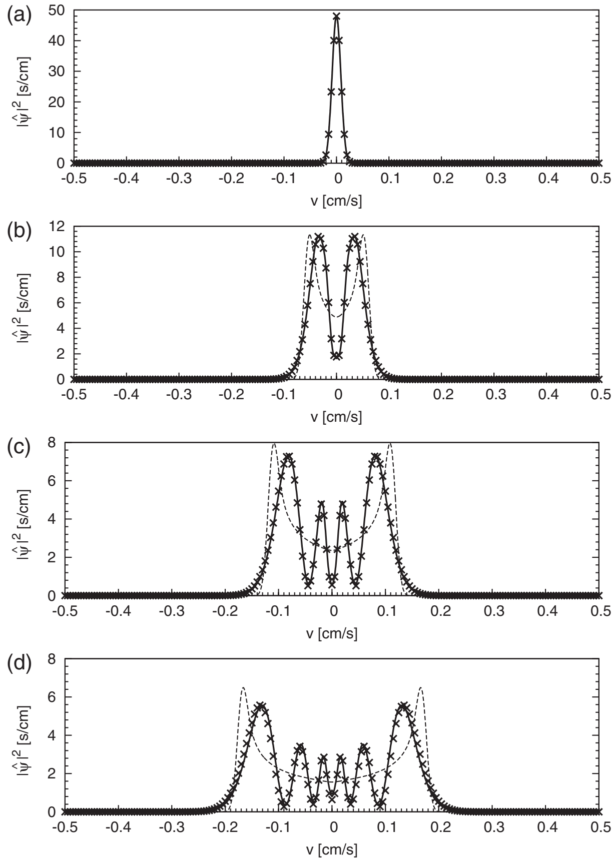

Fig. 1. Wave function in momentum space; exact result $|\hat{\psi}(t,v)|^2$ (lines), TF approximation $|\hat{\psi}_{TF}(t,v)|^2$ (crosses), classical result $P(t,v)$ (dashed lines); (a) $t=0$, (b) $t=0.2\,\mathrm{ms}$, (c) $t=0.4\,\mathrm{ms}$, (d) $t=0.6\,\mathrm{ms}$.

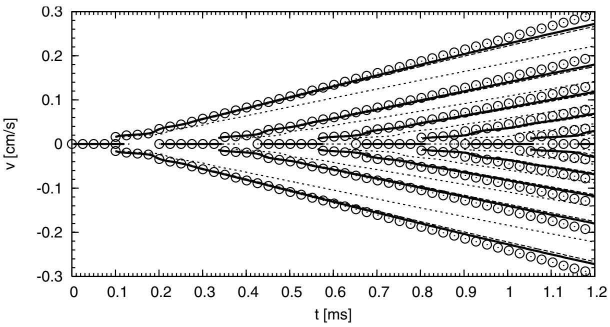

Fig. 2. Velocities of the peaks of the wave function $|\hat{\psi}(t,v)|^2$: $g_0=0$ (solid lines), $g_0=0.002344\,\mathrm{cm/s}$ (dashed lines), $g_0=0.02344\,\mathrm{cm/s}$ (dotted lines); TF approximation $|\hat{\psi}_{TF}(t,v)|^2$ (circles). In this and similar figures we always apply a threshold level such that the wave function is assumed to be zero if $|\hat{\psi}(v)|^2 < 0.001\max_{v'}|\hat{\psi}(v')|^2$.

function is the ground state of the 1D (stationary) Gross-Pitaevskii equation. We shall assume first that the initial interatomic interaction is zero (this will be relaxed later on). Then the Gross-Pitaevskii equation becomes a linear Schrödinger equation so that the ground state condensate wave function $\psi_0(x)$ is a Gaussian, namely

$$\psi_0(x) = \sqrt[4]{\frac{m\omega_x}{\pi\hbar}}\exp\left(-\frac{m\omega_x}{2\hbar}x^2\right), \tag{1}$$

where ω_x is the axial (angular) frequency. For the rest of the paper we choose $m = \mathrm{mass(Na)}$ and $\omega_x = 5/\mathrm{s}$.

Removing the trap under these conditions would preserve the momentum distribution, but if the interatomic interaction is immediately increased as the trap is removed, the momentum distribution evolution changes dramatically and in a highly non-classical way. If at time $t=0$ the confining trap is switched off and the interatomic interaction is switched on immediately (a more realistic switching procedure needing a finite time will be discussed below) then the time evolution is described by the time-dependent Gross-Pitaevskii equation,

$$i\hbar\frac{\partial\psi(t,x)}{\partial t} = -\frac{\hbar^2}{2m}\frac{\partial^2\psi(t,x)}{\partial x^2} + \frac{\hbar}{2}g_1\,|\psi(t,x)|^2\,\psi(t,x), \tag{2}$$

where g_1 is the effective 1D coupling parameter. We are examining short times $t < t_c := 1/(200\,\omega_x) = 1\,\mathrm{ms}$ (the factor $1/200$ is arbitrary, it should be true that $t \ll 1/\omega_x$) for which the absolute square of the Gaussian in equation (1) under the free evolution (i.e. Eq. (2) with $g_1=0$) is nearly not changing in coordinate space. Even with $g_1 = 234.4\,\mathrm{cm/s}$ and for times $t<1\,\mathrm{ms}$, the density profile $|\psi(t,x)|^2$ is nearly not changing. In contrast, during the early stage of the 1D expansion the momentum space distribution changes substantially: a time dependent interference occurs consisting of an orderly, one-by-one increase of the number of peaks, see Figure 1, with

$$\hat{\psi}(t,v) = \sqrt{\frac{m}{2\pi\hbar}}\int \mathrm{d}x\,\psi(t,x)\exp\left(-i\frac{vm}{\hbar}x\right).$$

The peak creation can be also seen in Figure 2 (solid lines), where the velocities of the peaks versus time are plotted forming a characteristic structure where bifurcations and creation of a new central peak follow each other. Remember that in the same period of time for the snapshots shown, the exact spatial profile has barely evolved from the initial one.

A way to make the momentum interference visible in coordinate space is to switch off the interatomic interaction again at a given time t_{off}. Then $|\hat{\psi}(v,t)|^2$ remains the same and therefore the position and number of peaks is not changing so that the subsequent free flight maps the momentum peaks into spatial ones. Therefore, for different times t_{off} a different peak pattern will appear in coordinate space (see Fig. 3) (solid lines). Only the central peak cannot be seen.

3 Origin of the interference pattern

To understand this effect better, we shall approximate equation (2). If we neglect the kinetic energy (TF regime) we get

$$i\hbar\frac{\partial}{\partial t}\psi_{TF}(t,x) = \frac{\hbar}{2}g_1\,|\psi_{TF}(t,x)|^2\,\psi_{TF}(t,x). \tag{3}$$

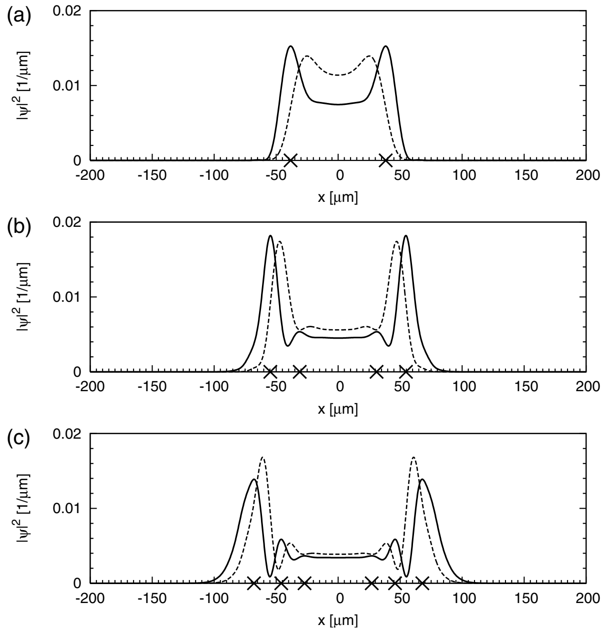

Fig. 3. Wave function in coordinate space; $t = 40\,$ms; $\Delta t = 0$ (solid lines), $\Delta t = 0.1\,$ms (dashed lines); the positions of the maxima are marked by crosses for $\Delta t = 0$; (a) $t_{off} = 0.2\,$ms, (b) $t_{off} = 0.4\,$ms, (c) $t_{off} = 0.6\,$ms.

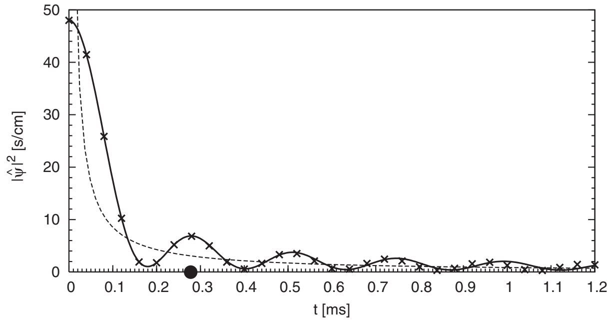

Fig. 4. Wave function in momentum space for $v = 0$: exact result $|\hat{\psi}(t,0)|^2$ (lines), TF approximation $|\hat{\psi}_{TF}(t,0)|^2$ (crosses), stationary-phase approximation $|\hat{\psi}_s(t,0)|^2$ (dashed line); the filled circle marks t_0.

For the simple step-like time dependence used here and for the free evolution we can write directly the solution $\psi_{TF}(t,x) = \psi_0(x)\exp(-it\,g_1|\psi_0(x)|^2/2)$. (For other analytical solutions of the Gross-Pitaevskii equation for trapped condensates with time-dependent trap parameters or coupling parameter see [16–18]. These works, however, study different regimes and not the interference effect discussed here.) In momentum space, we get

$$\hat{\psi}_{TF}(t,v) = \sqrt{\frac{m}{2\pi\hbar}}\sqrt[4]{\frac{m\omega_x}{\pi\hbar}}\int \mathrm{d}x\,\exp\left[-\frac{m\omega_x}{2\hbar}x^2 - \frac{i}{2}g_1 t\sqrt{\frac{m\omega_x}{\pi\hbar}}\exp\left(-\frac{m\omega_x}{\pi\hbar}x^2\right) - i\frac{vm}{\hbar}x\right]. \quad (4)$$

Note that in the TF regime the spatial density remains unchanged. The results for equation (4) are also plotted in Figures 1 and 2. There is a good agreement between the exact result and TF, and both show the same interference behaviour. It is clear that the nonlinearity is playing a key role in the effect.

We may compare the quantum dynamics with a similar classical one. Let us assume an ensemble of classical particles where the probability density of initial positions and velocities is given by $\rho_0(x,v) = |\psi_0(x)|^2|\hat{\psi}_0(v)|^2$, with $\psi_0(v)$ given by equation (1). The probability density is then evolved with the classical Liouville equation with the Hamiltonian $H = \frac{\hbar}{2}g_1\int dv'\rho_t(x,v')$, without kinetic term in analogy to the quantum Hamiltonian of the TF regime, see equation (3). The solution is given by $\rho_t(x,v) = \rho_0(x, v+\alpha t)$ with $\alpha = \frac{\hbar}{2}\frac{g_1}{m}\frac{\partial}{\partial x}\int \mathrm{d}v\,\rho_0(x,v)$. $P(t,v) := \int \mathrm{d}x\,\rho_t(x,v)$ is also plotted in Figure 1. The classical picture provides, approximately, the outer peaks moving outwards with time because of the release of potential energy, but not the central ones, which are therefore associated with quantum interference. Let us examine this interference.

Defining dimensionless quantities $\zeta = \sqrt{m\omega_x/\hbar}\,x$, $\tau = \sqrt{m\omega_x/\hbar}\,g_1 t$, and $\kappa = \sqrt{m/\hbar\omega_x}\,v$, we write equation (4) as

$$\hat{\psi}_{TF}(\tau,\kappa) = \frac{1}{\sqrt{2\pi\omega_x}}\sqrt[4]{\frac{m\omega_x}{\pi\hbar}} \times \int \mathrm{d}\zeta\,\exp\left[-\frac{\zeta^2}{2} - i\tau\left(\frac{1}{2\sqrt{\pi}}e^{-\zeta^2} + \frac{\kappa}{\tau}\zeta\right)\right]. \quad (5)$$

An important characteristic time is the value τ_0 when the second maximum of $|\hat{\psi}_{TF}(\tau_0,\kappa\equiv 0)|^2$ in the TF approximation appears (the first maximum is at $\tau = 0$), see Figure 4. This sets the scale of the oscillations and the value is found numerically,

$$\tau_0 \approx 27.703 \quad\Rightarrow\quad t_0 \approx \frac{27.703}{g_1}\sqrt{\frac{\hbar}{m\omega_x}}.$$

This time t_0 should be much smaller than the critical time t_c when the kinetic energy starts to influence. Therefore we get a necessary condition for g_1,

$$t_c = \frac{1}{200\,\omega_x} > t_0 \approx \frac{27.703}{g_1}\sqrt{\frac{\hbar}{m\omega_x}} \Rightarrow g_1 > 27.703\times 200\sqrt{\frac{\hbar\omega_x}{m}} \approx 65.12\,\mathrm{cm/s}.$$

We will simplify further equation (5) by means of the stationary phase method. If κ/τ is constant and $\tau\to\infty$ then the main contribution to the integral (5) comes from the values ζ which fulfil

$$\frac{\partial}{\partial\zeta}\left[\frac{1}{2\sqrt{\pi}}e^{-\zeta^2} + \frac{\kappa}{\tau}\zeta\right] = 0 \;\Rightarrow\; -\zeta\frac{e^{-\zeta^2}}{\sqrt{\pi}} + \frac{\kappa}{\tau} = 0.$$

If $0 < |\kappa/\tau| < \exp(-1/2)/\sqrt{2\pi}$ there are two solutions ζ_0, ζ_1 with $0 < |\zeta_0| < 1/\sqrt{2} < |\zeta_1|$. Physically these are

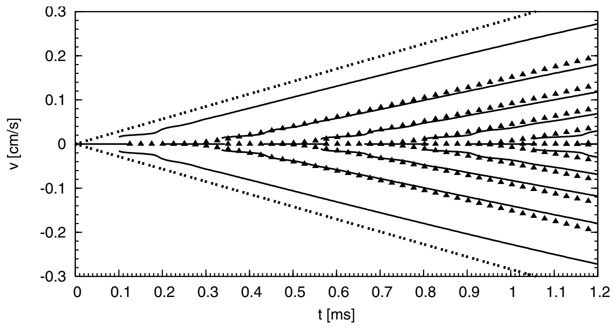

Fig. 5. Velocities of the peaks of the exact result $|\hat{\psi}|^2$ (lines), the stationary-phase approximation $|\hat{\psi}_s|^2$ (triangles); the outer thick-dotted lines mark the critical values $\pm v_c(t)$.

two positions in which the force exerted on the atom is equal because the Gaussian profile of the potential changes from concave-down around the centre, to concave-up in the tails. Thus these two positions contribute to the same momentum and the corresponding amplitudes will interfere quantum mechanically. The stationary phase approximation of equation (5) is

$$\hat{\psi}_s(\tau,\kappa) = \sqrt[4]{\frac{m\omega_x}{\hbar}} e^{i\frac{\pi}{4}} \frac{1}{\sqrt{\tau\omega_x}} \times \left\{ \frac{\exp\left[-i\tau(\frac{e^{-\zeta_0^2}}{2\sqrt{\pi}} + \frac{\kappa}{\tau}\zeta_0)\right]}{\sqrt{1-2\zeta_0^2}} - i\frac{\exp\left[-i\tau(\frac{e^{-\zeta_1^2}}{2\sqrt{\pi}} + \frac{\kappa}{\tau}\zeta_1)\right]}{\sqrt{2\zeta_1^2-1}} \right\}. \tag{6}$$

Figure 5 shows also the peaks of $|\hat{\psi}_s(\tau,\kappa)|^2$ resulting from using equation (6) in the range $0 < |\kappa/\tau| < \exp(-1/2)/\sqrt{2\pi}$. Except for the outer peaks and the $\kappa = 0$ line, equation (6) gives the correct peak behaviour. The opening of the cone of the effect can be approximated by the definition of a critical $\kappa_c(\tau)$ or $v_c(t)$ to make the interference possible,

$$\frac{\kappa_c}{\tau} = \frac{\exp(-1/2)}{\sqrt{2\pi}} \;\Rightarrow\; \kappa_c(\tau) = \frac{\exp(-1/2)}{\sqrt{2\pi}}\tau,$$

or $v_c(t) = \exp(-1/2)\omega_x g_1 t/\sqrt{2\pi}$, see also Figure 5.

4 Stability

Up to now we have considered an abrupt switching of the interaction, but the effect remains for switching times Δt even of the order of t_0. For a time dependent coupling parameter given by

$$g(t) = g_1 \times \begin{cases} 0 & : \; t \le 0 \text{ or } t \ge t_{off} \\ 1 & : \; \Delta t \le t \le t_{off} - \Delta t \\ f(t) & : \; 0 < t < \Delta t \\ f(t_{off} - t) & : \; t_{off} - \Delta t < t < t_{off} \end{cases}, \tag{7}$$

with $f(t) = (t/\Delta t)^2(3 - 2t/\Delta t)$, the result for $\Delta t = 0.1$ ms is shown in Figure 3: the effect is not changing qualitatively, only the positions of the peaks are squeezed.

We have also examined the stability with respect to a non-zero value of the coupling constant used to prepare the initial state, g_0. The initial ground state is then no longer a Gaussian and can only be calculated numerically. The effect survives as long as $g_0 \ll g_1$ but the interference pattern is again squeezed, see Figure 2.

5 Three-dimensional effect

The preparation of the condensate may also be carried out in a spherical-symmetric harmonic trap $V(\boldsymbol{r}) = m\omega^2 r^2/2$. With negligible interatomic interaction strength, the ground state is again approximately Gaussian, namely

$$\psi_{0,3d}(\boldsymbol{r}) = \left(\frac{m\omega}{\pi\hbar}\right)^{3/4} e^{-\frac{m\omega r^2}{2\hbar}}. \tag{8}$$

After switching off the trap and switching on the interaction $\tilde{g}_1$, the 3D time-dependent Gross-Pitaevskii equation is given by

$$i\hbar\frac{\partial}{\partial t}\psi_{3d}(t,\boldsymbol{r}) = -\frac{\hbar^2}{2m}\Delta\psi_{3d} + \frac{\hbar}{2}\tilde{g}_1 \left|\psi_{3d}(t,\boldsymbol{r})\right|^2 \psi_{3d}\,. \tag{9}$$

We assume that we can neglect the kinetic part. In this Thomas-Fermi regime, the solution of equation (9) with initial condition (8) is

$$\psi_{3d}(t,\boldsymbol{r}) = \psi_{0,3d}(\boldsymbol{r}) \exp\left(-\frac{i}{2}t\,\tilde{g}_1 \left|\psi_{0,3d}(\boldsymbol{r})\right|^2\right)$$

or in momentum representation

$$\begin{aligned}\hat{\psi}_{3d}(t,\boldsymbol{v}) &= \left(\frac{m}{2\pi\hbar}\right)^{3/2} \int \mathrm{d}^3\boldsymbol{r}\,\psi_{3d}(t,\boldsymbol{r})\,e^{-i\frac{m\boldsymbol{v}}{\hbar}\boldsymbol{r}} \\ &= i\left(\frac{m\omega}{\pi\hbar}\right)^{3/4} \sqrt{\frac{m}{2\pi\hbar}}\frac{1}{v}\int_{-\infty}^{\infty}\mathrm{d}r\,r \\ &\times \exp\left[-\frac{m\omega}{2\hbar}r^2 - i\frac{mv}{\hbar}r - \frac{i}{2}t\,\tilde{g}_1\left(\frac{m\omega}{\pi\hbar}\right)^{3/2} e^{-\frac{m\omega}{\hbar}r^2}\right].\end{aligned}$$

We introduce the dimensionless variables $\zeta = \sqrt{m\omega/\hbar}\,r$, $\vec{\kappa} = \sqrt{m/\hbar\omega}\,\boldsymbol{v}$, and $\tau = \sqrt{\pi}\,(m\omega/\pi\hbar)^{3/2}\,t$ and get

$$\hat{\psi}_{3d}(\tau,\vec{\kappa}) = \frac{i}{2\pi}\left(\frac{m}{\pi\hbar\omega}\right)^{3/4} \times \frac{1}{\kappa}\int_{-\infty}^{\infty}\mathrm{d}\zeta\,\zeta\,\exp\left[-\frac{\zeta^2}{2} - i\kappa\left(\frac{1}{2\sqrt{\pi}}e^{-\zeta^2} + \frac{\kappa}{\tau}\zeta\right)\right]. \tag{10}$$

Note that equation (10) has nearly the same structure of the corresponding one-dimensional one (5). For a better comparison of the one- and three-dimensional cases we define the one-dimensional probability density

$$\begin{aligned}\rho_{1d}(\tau,\kappa) &:= 2\sqrt{\frac{\hbar\omega_x}{m}}\left|\hat{\psi}_{TF}(\tau,\kappa)\right|^2 \\ &= \frac{1}{\pi^{3/2}}\left|\int d\zeta\,\exp\left[-\frac{\zeta^2}{2} - i\tau\left(\frac{1}{2\sqrt{\pi}}e^{-\zeta^2} + \frac{\kappa}{\tau}\zeta\right)\right]\right|^2\end{aligned}$$

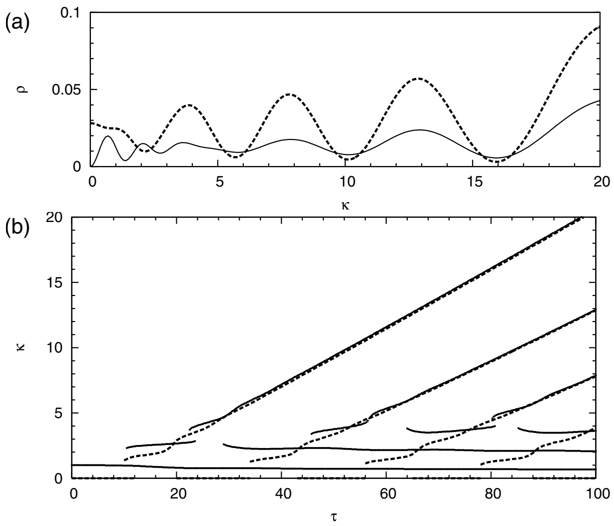

Fig. 6. (a) Probability densities ρ_{1d} (dashed line) and ρ_{3d} (solid line) for $\tau = 100$; (b) Velocities κ of the peaks of the probability densities ρ_{1d} (dashed lines) and ρ_{3d} (solid lines).

and the three-dimensional one

$$\rho_{3d}(\tau,\kappa) := \left(\frac{\hbar\omega}{m}\right)^{3/2} \times \kappa^2 \int_0^{2\pi} \mathrm{d}\varphi \int_0^{\pi} \mathrm{d}\Theta \sin\Theta \left|\hat{\psi}_{3d}(t, \vec{\kappa}\ (\kappa,\varphi,\Theta))\right|^2 = \frac{1}{\pi^{3/2}} \left| \int \mathrm{d}\zeta\, \zeta\, \exp\left[-\frac{\zeta^2}{2} - i\tau\left(\frac{1}{2\sqrt{\pi}} e^{-\zeta^2} + \frac{\kappa}{\tau}\zeta\right)\right]\right|^2.$$

Both expressions give the probability density to measure a velocity of absolute value $\kappa > 0$ at time τ and they are normalised such that $\int_0^\infty \mathrm{d}\kappa\, \rho_{1d/3d}(\tau,\kappa) = 1$. In Figure 6, we compare these two functions and the velocities κ of the peaks. It can be clearly seen that we get basically the same interference effect, namely an orderly, one-by-one increase of the number of peaks in the momentum distribution. Moreover, for larger values of κ the velocities of the maxima actually coincide in both one and three dimensions.

6 Summary

Summarising, we have examined the short-time behaviour of a Bose-Einstein condensate when the interatomic interaction is negligible for the preparation in the harmonic trap, and strongly increased when the potential trapping is removed. We have found a quantum interference effect in momentum space originated from the interatomic interaction change. The momentum distribution expands due to the release of mean field energy and the number of peaks increases with time because of the interference of two positions in coordinate space contributing to the same momentum. The effect is stable in a parameter range and could be observed with current technology.

We are grateful to C. Salomon for encouragement at an early stage of the project, and to G. García-Calderón for commenting on the manuscript. This work has been supported by Ministerio de Educación y Ciencia (BFM2003-01003) and UPV-EHU (00039.310-15968/2004). A.C. acknowledges financial support by the Basque Government (BFI04.479).

References

1. W. Ketterle, D.S. Durfee, D.M. Stamper-Kurn, in *Bose-Einstein condensation in atomic gases*, edited by M. Inguscio, S. Stringari, C.E. Wieman (IOS Press, Amsterdam, 1999), pp. 67-176
2. P. Öhberg, L. Santos, Phys. Rev. Lett. **89**, 240402 (2002)
3. S. Dettmer, D. Hellweg, P. Ryytty, J.J. Arlt, W. Ertmer, K. Sengstock, D.S. Petrov, G.V. Shlyapnikov, H. Kreutzmann, L. Santos, M. Lewenstein, Phys. Rev. Lett. **87**, 160406 (2001)
4. S. Chen, R. Egger, Phys. Rev. A **68**, 063605 (2003)
5. A. del Campo, J.G. Muga, Europhys. Lett. **74**, 965 (2006)
6. P. Villain, M. Lewenstein, Phys. Rev. A **62**, 043601 (2000)
7. J. Stenger, S. Inouye, A.P. Chikkatur, D.M. Stamper-Kurn, D.E. Pritchard, W. Ketterle, Phys. Rev. Lett. **82**, 4569 (1999)
8. L. Pitaevskii, S. Stringari, Phys. Rev. Lett. **83**, 4237 (1999)
9. M.R. Andrews, C.G. Townsend, H.-J. Miesner, D.S. Durfee, D.M. Kurn, W. Ketterle, Science **275**, 637 (1997)
10. K. Bongs, S. Burger, G. Birkl, K. Sengstock, W. Ertmer, K. Rzążewski, A. Sanpera, M. Lewenstein, Phys. Rev. Lett. **83**, 3577 (1999)
11. A. Pérez, S. Brouard, J.G. Muga, Phys. Rev. A **64**, 012710 (2001)
12. S. Inouye, M.R. Andrews, J. Stenger, H.-J. Miesner, D.M. Stamper-Kurn, W. Ketterle, Nature **392**, 151 (1998)
13. M. Theis, G. Thalhammer, K. Winkler, M. Hellwig, G. Ruff, G. Grimm, J. Hecker Denschlag, Phys. Rev. Lett. **93**, 123001 (2004)
14. D. Hellweg, S. Dettmer, P. Ryytty, J.J. Arlt, W. Ertmer, K. Sengstock, D.S. Petrov, G.V. Shlyapnikov, H. Kreutzmann, L. Santos, M. Lewenstein, Appl. Phys. B **73**, 781 (2001)
15. H. Kreutzmann, A. Sanpera, L. Santos, M. Lewenstein, D. Hellweg, L. Cacciapuoti, M. Kottke, T. Schulte, K. Sengstock, J.J. Arlt, W. Ertmer, Appl. Phys. B **76**, 165 (2003)
16. Yu. Kagan, E.L. Surkov, G.V. Shlyapnikov, Phys. Rev. A **54**, R1753 (1996)
17. Yu. Kagan, E.L. Surkov, G.V. Shlyapnikov, Phys. Rev. A **55**, R18 (1997)
18. Yu. Kagan, E.L. Surkov, G.V. Shlyapnikov, Phys. Rev. Lett. **79**, 2604 (1997)